Revised August 10, 2001. Original published in New Technological and Design Developments in Deep Foundations, Proceedings of GeoDenver 2000, Norman D. Dennis, Jr., Ray Castelli, and Michael W. O'Neill, Eds., Geotechnical Special Publication, ASCE Press, Reston, VA

Energy Method for Predicting Installation Torque of Helical Foundations and Anchors

Howard A. Perko, PE, Associate Member[1]

Abstract

A theoretical model is developed to support the well known empirical relationship between capacity and torque for helical foundations and anchors. The model is based on energy exerted during installation and that required to displace the helical foundation or anchor once in place. Through the equivalence of energy, the model relates bearing and pullout capacity directly to installation torque. Downward force during installation, helical blade geometry, multiple helices, blade pitch per revolution, and hub radius are taken into account.

The model is applied to determine the capacity and installation torque for several helical foundations and anchors of different geometric configurations. Theoretical predictions are shown to correlate with previously published field and laboratory measurements.

Introduction

Helical foundation and anchor capacity has been empirically related to installation torque (Hoyt and Clemence, 1989). The coefficient of proportionality, K, between capacity and torque is known to vary for helical foundations and anchors of different geometric configurations. Previous research indicates that K may depend on depth (Ghaly, Hanna, and Hanna, 1991b). Other research indicates that K is independent of helical blade radius and highly dependent on hub diameter (Hoyt and Clemence, 1989). Still other literature indicates that K is weakly correlated with number of helical blades (Hargrave and Thorsten, 1992).

In addition to the empirical method involving installation torque, the capacity of a helical foundation or anchor (also commonly called a helix pier) can be estimated by two different methods of limit state analysis. One method involves failure of a cone or cylinder of soil surrounding and above the helices, while the other involves individual bearing capacity failure of each helix (Ghaly and Clemence, 1998; A.B.Chance, Co., 1995; Ghaly, Hanna and Hanna, 1991a; Rao, Prasad, and Veeresh, 1993; Mitsch and Clemence, 1985; Rao, Prasad, and Shetty, 1991; Clemence and Pepe, 1984; Hoyt and Clemence, 1989; Ghaly, Hanna, and Hanna, 1991b; and Rao and Prasad, 1993). The

[1]Manager, Secure Products, LLC, 727 Laporte Ave., Ft. Collins, CO 80521
howie@engr.colostate.edu, phone: 970-472-5068, fax: 970-472-0264

difficulty with limit state analysis for helix piers is that it requires prior knowledge of the soil strength and the ability to determine the probable mode of failure.

Torque measurements taken during installation of a helix pier are indicators of soil shear strength at the depth through which the helical blades are passing. Due to the complex interaction of the blades with the soil, it is difficult to relate torque measurements with angle of friction and cohesion of the soil. In order to avoid this difficulty, a model is proposed, wherein the capacity of a helix pier is directly related to the installation torque by energy equivalence. This method accounts for downward pressure during installation, helical blade geometry, multiple helices, blade pitch per revolution, and hub radius. Predictions based on the model are compared with data from previous studies.

Model Derivation

The energy model for predicting helix pier capacity/torque relationships is based on the following postulate.

Postulate: For local shear, penetration energy is proportional to the volume of soil displaced times the distance displaced.

Justification for this postulate is derived from the characteristic soil stress-displacement function shown in Fig. 1. The initial portion of this function is approximately linear. A new constitutive parameter, P, is defined as the slope of the stress-displacement function. Penetration energy is simply

$$E_{penetration} = \int_0^{\delta} \sigma A d\delta' \qquad \textbf{(1)}$$

where δ' is displacement, δ is final displacement, σ is stress, and A is penetrator area. Replacing σ in Eq. (1) by Pδ and integrating results in

$$E_{penetration} = \frac{1}{2} P A \delta^2 \qquad \textbf{(2)}$$

Since area times displacement is just the volume of soil displaced, Aδ can be replaced by ΔV and the penetration energy is

$$E_{penetration} = \frac{1}{2} P \delta \Delta V \qquad \textbf{(3)}$$

Thus, the penetration energy is proportional to the volume of soil displaced times the distance displaced. The proportionality factor, P, is constant for small displacements typical of local shear.

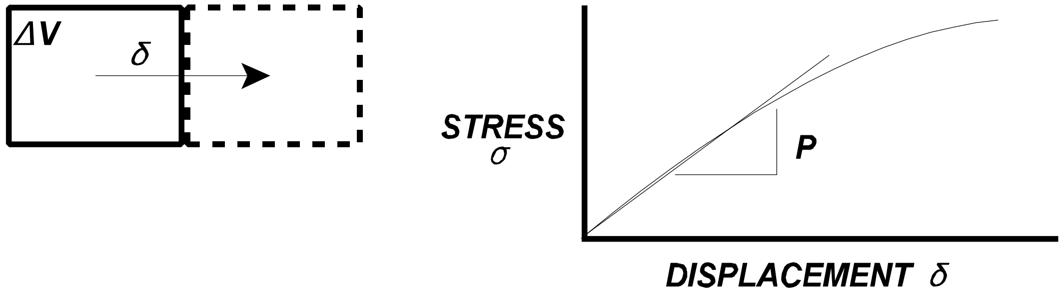

Fig. 1 Typical Soil Stress-Displacement Function

The first step in the derivation of the energy model is to determine the constitutive parameter, P. This was accomplished by equating the energy exerted during installation of a helix pier with the appropriate penetration energy and losses due to friction.

$$E_{installation} = E_{penetration} + E_{losses} \tag{4}$$

Helix pier installation typically involves rotating the pier into the ground and applying a downward force. Energy required to rotate an object is equal to the torque times the angle of rotation. Energy exerted by the downward force is just the force times the distance over which the force acts. For one full rotation, the downward distance moved is equal to the pitch of the blades. Thus, installation energy per revolution is given by

$$E_{installation} = 2\pi T + Fp \tag{5}$$

where T is torque, F is downward force, and p is pitch.

Penetration energy can be determined according to Eq. (3). For one revolution, the volume of soil displaced by the helix pier is equal to the sum of the volumes of all the individual cutting blades plus the volume of soil displaced by the hub in moving downward the distance of the pitch, as shown in Fig. 2. Provided the pitch is small, the volume of a helical plate is nearly the same as the volume of a circular plate with the same radius. Furthermore, as a penetrator moves through the soil, the soil is split and displaced to sides. As shown in Fig. 3, the average distance, *, required to displace the soil for helical blade insertion is approximately equal to half the thickness of the blades. Whereas, for hub penetration, this distance is approximately equal to the radius of the hub. Hence, the penetration energy for helix pier installation from Eq. (3) is given by

$$E_{penetration} = \frac{\pi}{4} P[\ 2r^3 p + \sum_n (R_n^2 - r^2) t_n^2\ ] \tag{6}$$

where n is the number of cutting blades and the other parameters are defined in Fig. 2.

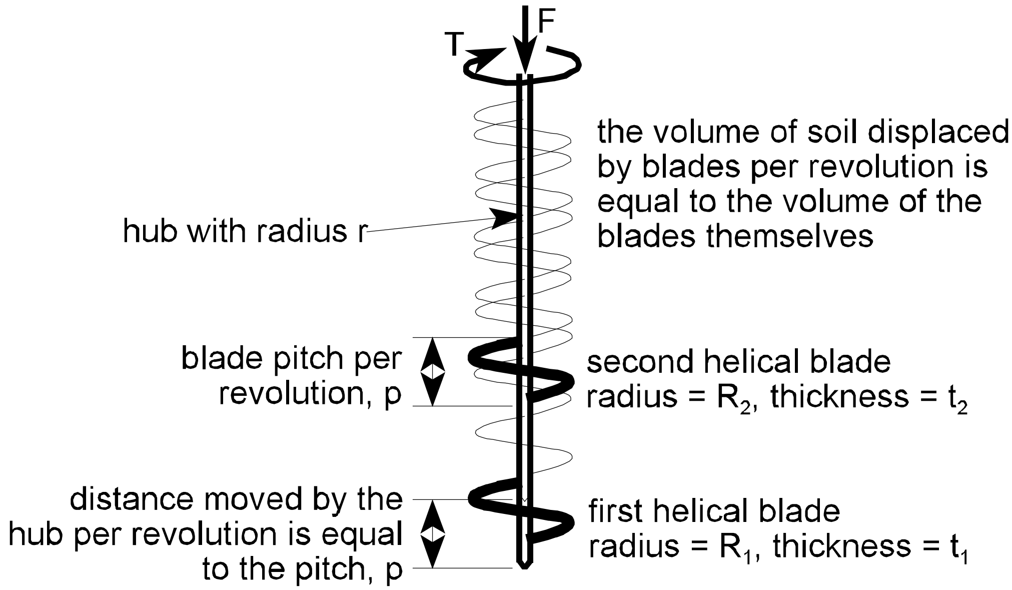

Fig. 2 Helix Pier Installation

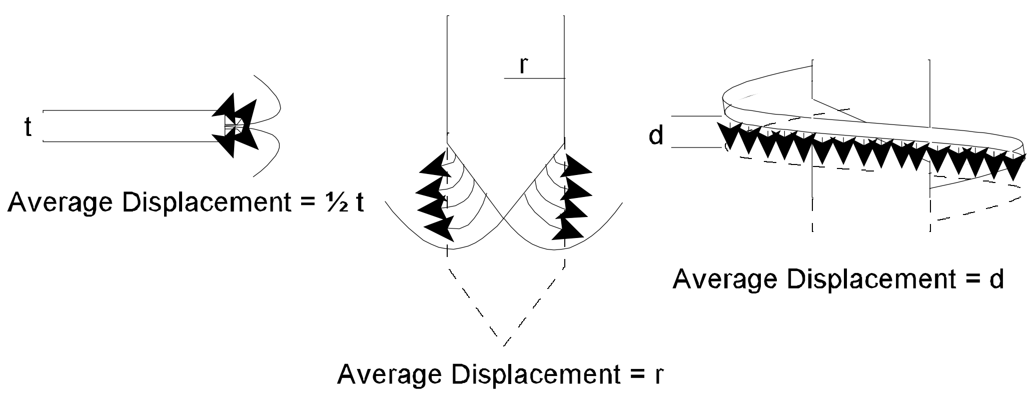

Fig. 3 Various Displacement Distances

Energy losses due to friction can be estimated by converting soil shear stress into torque and multiplying by the angle of twist, 2B. As the helix pier is being turned in the ground, soil shear stress is mobilized along the helical blades and hub. The shear stress developed is a fraction, ", of the penetration stress, F. Torque due to shear along the hub is "F times the surface area of the hub and the moment arm (r). Wobbling often causes the recession of upper soils from around the hub, therefore it is suggested that the length of hub experiencing friction be limited to a length represented by 8. For square hubs, which push most of the soil away, 8 is approximately equal to the pitch, p. Torque due to the blades is "F times the sum of the blade surface areas times the moment arm. Since the surface area and consequently the shear force increase by r^2, the moment arm for the resultant force is equal to the distance to the geometric centroid of a paraboloid, given by 2/3 R. Therefore, the energy loss due to friction upon one revolution of a helix pier is given by

$$E_{losses} \ = \ \frac{4}{3}\pi^2\sigma\alpha[\ 3r^2\lambda \ + \ 2\sum_m (R_m^3 - r^3)\ ] \tag{7}$$

where m is the total number of blades even if they follow the same path. However, F can be replaced by P* in accordance with the penetration energy postulate. By incorporating the appropriate values of * for the blades and the hub, Eq. (7) can be written in the form

$$E_{losses} \ = \ \frac{4}{3}\pi^2 P\alpha[\ 3r^3\lambda \ + \ \sum_m (R_m^3 - r^3)t_m\ ] \tag{8}$$

The constitutive parameter, P, can be found by incorporating Eqs. (5), (6), and (8) into Eq. (4) and solving for P in terms of torque.

The next step in the derivation of the model is to formulate an equation for the capacity of a helix foundation or anchor in terms of P. There are two predominant methods of determining helix foundation or anchor capacity based on limit state analysis. Limit state conditions can require considerable displacements in order to mobilize shear strength and for general bearing capacity failure. For practical purposes, the allowable movement of foundations and anchors is typically limited to small displacements. The capacity for small displacements can be determined using the penetration energy postulate and an energy balance between the energy exerted during loading and the appropriate penetration energy of each of the supporting blades.

$$E_{loading} \ = \ E_{penetration} \tag{9}$$

In Eq. (9), it is assumed that energy losses due to friction along the hub are negligible, because only a fraction of the shear strength is mobilized for small displacements. Also, the capacity in uplift is approximately equal to the bearing capacity, since small movements in either the upward or downward direction should only depend on the effective confining stress around the blades.

The energy during loading can be determined by integrating the applied force over a specific helix pier displacement. For a linear force-displacement function, the energy during loading is given by

$$E_{loading} \ = \ \frac{1}{2}Qd \tag{10}$$

where Q is the final capacity and d is the vertical movement.

Penetration energy during loading can be determined according to Eq. (3). The volume of soil displaced by the helix pier is equal to the sum of the areas of the blades and the end area of the hub times the displacement distance, d. This assumes that the end of the hub is closed to prohibit soil entry. Penetration energy is given by

$$E_{penetration} \ = \ \frac{\pi}{2}Pd^2\ [\ r^2 \ + \ \sum_m (R_m^2 - r^2)\ ] \tag{11}$$

Substitution of Eqs. (10) and (11) and the result for P from step one into Eq. (9) yields an expression for capacity in terms of installation torque, applied downward force, pier displacement, and the geometry of the helix pier, given by

$$Q = \frac{12d(2\pi T + Fp)[r^2 + \sum_m (R_m^2 - r^2)]}{3[2r^3 p + \sum_n (R_n^2 - r^2)t_n^2] + 16\pi\alpha[3r^3\lambda + \sum_m (R_m^3 - r^3)t_m]} \tag{12}$$

Model Comparison

The model was compared with capacity-torque ratios found empirically by Hoyt and Clemence (1989). Their study involved anchors with 1-1/2, 1-3/4, and 2-in square hubs and 3-1/2 and 8-5/8-in diameter round hubs. The number of helices varied from 2 to 14, and their diameters varied from 6 to 20 in. According to Hoyt and Clemence, the capacity/torque ratio depends predominantly on the diameter of the hub. The ratio is believed to be largely independent of number of helical blades and helix diameter. They found an average capacity/torque ratio, K, equal to 10 ft^{-1} for all square hub anchors that were tested, 7 ft^{-1} for the 3-1/2-in diameter round-hub anchors, and 3 ft^{-1} for the 8-5/8-in diameter round-hub anchors.

The actual configurations of the helix piers studied by Hoyt and Clemence is proprietary information and could not be obtained. Consequently, it was necessary to assume a variety of helix pier configurations as shown in Table 1. The ratio of side shear to penetration stress, ", was set equal to 0.6, the effective hub length, 8, was set equal to the blade pitch, and the displacement at failure, d, was assumed to equal 1 in. Results of the model match Hoyt and Clemence fairly well. A capacity/torque ratio, K, of approximately 11, 8, and 1 ft^{-1} were obtained for square hub anchors, the 3-1/2-in diameter round-hub anchors, and the 8-5/8-in diameter round-hub anchors, respectively. This ratio is independent of blade pitch, number of helices, downward force applied during installation, and final installation torque.

The model predicts that K decreases with increasing values of R, which is contrary to the findings of Hoyt and Clemence. The model also predicts a decrease in K with increasing hub radius, r, which is consistent with the findings of Hoyt and Clemence. Model predictions are a helix pier displacement of 1 inch. It is unknown whether what displacement was used to designate failure in the study by Hoyt and Clemence.

To further verify the model, it was compared with other previously published field and laboratory data. Using descriptions of the helix pier geometries from the literature, the model was used to calculate theoretical capacity/torque ratios. Model predictions are compared with actual measured values in Fig. 4. The diagonal line in the figure represents a 1:1 correlation between predicted and measured capacity/torque ratio, K. As described in the legend on the right side of the figure, the helix piers tested in previous literature have a variety of sizes and styles. Measured values of K ranged from 4 to 39 ft^{-1}. Predicted values of K based on the model match the general range and trend of field measurements quite well. The fact that model predictions compare well with measurements for a wide variety of helix pier sizes and geometries from small scale laboratory models to full scale field tests indicates that the energy method for torque to capacity ratio determination has merit as a first approximation.

Table 1. Example Capacity/Torque Ratio Model Predictions

Number of Cutting Blades n	Total Number of Blades m	Blade Radius R *(in)*	Hub Radius r *(in)*	Blade Pitch p *(in/rev)*	Effective Hub Length 7 *(in)*	Blade Thickness t *(in)*	Capacity to Torque Ratio K *(ft^{-1})*
1	1	6	1.1	2.0	3	0.375	11.8
1	1	6	1.1	3.0	3	0.375	11.8
1	1	6	1.1	4.0	3	0.375	11.8
1	1	6	1.1	5.0	3	0.375	11.8
1	1	6	1.1	3.0	3	0.375	11.8
2	2	6	1.1	3.0	3	0.375	12.4
3	3	6	1.1	3.0	3	0.375	12.6
4	4	6	1.1	3.0	3	0.375	12.7
1	1	4	1.1	3.0	3	0.375	13.7
1	1	5	1.1	3.0	3	0.375	13.0
1	1	6	1.1	3.0	3	0.375	11.8
1	1	7	1.1	3.0	3	0.375	10.6
1	1	6	1.1	3.0	3	0.375	11.8
1	1	6	1.1	3.0	3	0.5	9.1
1	1	6	1.1	3.0	3	0.75	6.2
1	1	6	1.4	3.0	3	0.375	10.2
1	1	6	1.6	3.0	3	0.375	9.1
1	1	6	1.8	3.0	3	0.375	8.0

The diamond symbol in Fig. 4 represents an field test by Rupiper and Edwards (1989), which consisted of measuring the installation torque and bearing capacity of a square-hub helix pier with a single 14-in diameter helical blade. According to their paper, the pier exhibited a maximum capacity at a displacement of only 0.15 in. Both the model and the field test indicate a low capacity to torque ratio for such a small displacement.

The open circle symbols in the figure correspond to a laboratory investigation that was performed by Ghaly, Hanna, and Hanna (1991) which involved uplift capacity testing of several small helix anchors. Each anchor had a round hub with a single 2-in diameter helical blade. Blade pitch varied from 3/8 to 3/4 inch per revolution. Installation torque varied from 17 to 30 ft-lbs. The model indicates a weak dependance of K on pitch and generally matches the laboratory results. Their investigation also included unsymmetrical and parallel-blade, variable-pitch anchors. It is considerably more difficult to apply the model to these types of anchors; consequently, they were not analyzed.

Referring again to Fig. 4, the open triangle symbols represent full scale field tests performed by Mitsch and Clemence (1985) on square hub piers with triple 11-in diameter helical blades, while the open square symbols represent laboratory tests performed by the same investigators on 1/3 scale models. Some of the models had uniform diameter triple helical blades. Others had single blades. The model predicts nearly the same value of K for single and multiple blade helix pier geometries. Most of the variations in K predicted by the model are the result of different values of measured helix pier displacement. For example, the set of open square symbols on the left side of the graph correspond to helix piers that reached peak capacity at a displacement of about 0.1 in, while the same symbols in the middle of the graph correspond to helix pier displacements of 0.2 in and the same symbols near the top right corner of the graph correspond to helix pier displacements of 0.4 in.

Another set of data in Fig. 4, shown by the star symbols, are associated with field tests performed by Hargrave and Thorsten (1992) using square hub helix piers with single 10-in diameter helical blades. The model matched the results of their field tests with nearly 1:1 correspondence. Field tests were also conducted on helix piers with multiple radii, double blades, and again these data were omitted to avoid complexity. These more complicated geometries will be the subject of a forthcoming theoretical study not yet completed.

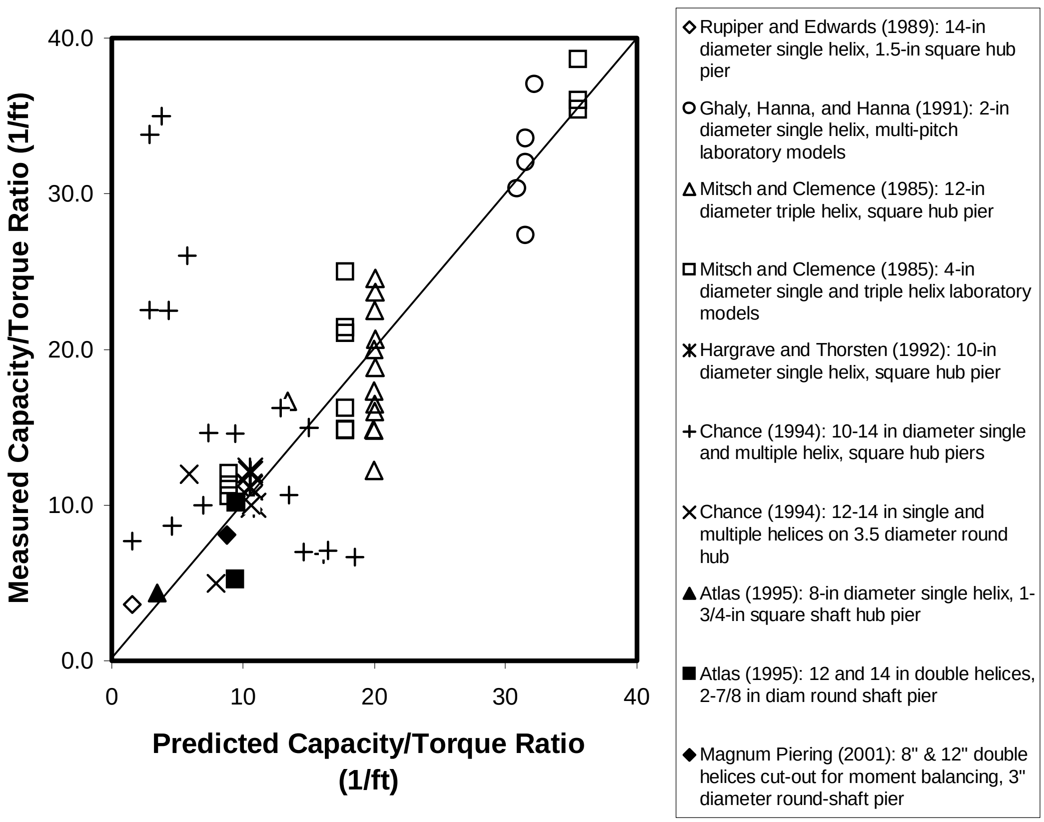

Fig. 4 Model Comparison with Measured Values

Discussion

As a point of clarification, the difference between the number of cutting blades, n, and the total number of blades, m, has to do with whether or not the blades are mounted to the hub in a manner that allows each blade to follow the path cut by the foregoing blade. If each blade cuts its own path through the soil then n is equal to m.

In practical applications, helical blades do not often follow the path cut by one another due to accidental augering and slipping during installation.

In applying the model, the effective length of the hub was assumed to equal the pitch of the helical blades. For square shaft helix piers, this assumption is based on the square hub creating a round hole and displacing the soil away from the hub within one revolution. For round-shaft helix piers, the value of 8 is less evident. The magnitude of predicted values of K has a significant dependance on the effective hub length, 8, that is assumed. Larger values of 8 correspond with smaller values of K. As consistent with square-shaft hubs, a value of 8 equal to the blade pitch provides the closest match to the K value measured by Hoyt and Clemence and in other field tests. This indicates that much of the soil separates from the hub during installation due to wobbling.

In developing the model, the friction generated along the blades and sides of the hub during installation was assumed to be proportional to the penetration resistance, and a proportionality factor, ", was introduced. For the model predictions presented herein, " was set equal to 0.6. Justification for this value is based on the following.

As the soil moves to the side to allow for helical blade insertion, the penetration resistance, F, is left acting in a direction approximately normal to the surface of the blade, as shown in Fig. 5. The penetration resistance is the major principle stress in the soil about the helical blades and leading end of the hub during installation. If the friction angle between galvanized steel and soil is 30 degrees, then the friction generated along the blades and hub is equal to 0.6 F. Note that this does not require the assumption that F is uniform. Instead, F is related to the distance of soil displacement and the volume of soil displaced during penetration in accordance with Eq. (1). There may be some dependence of " and K on soil consistency, but this dependence is expected to be small because the friction coefficient between steel and soil is largely independent of soil density (Das, 1990).

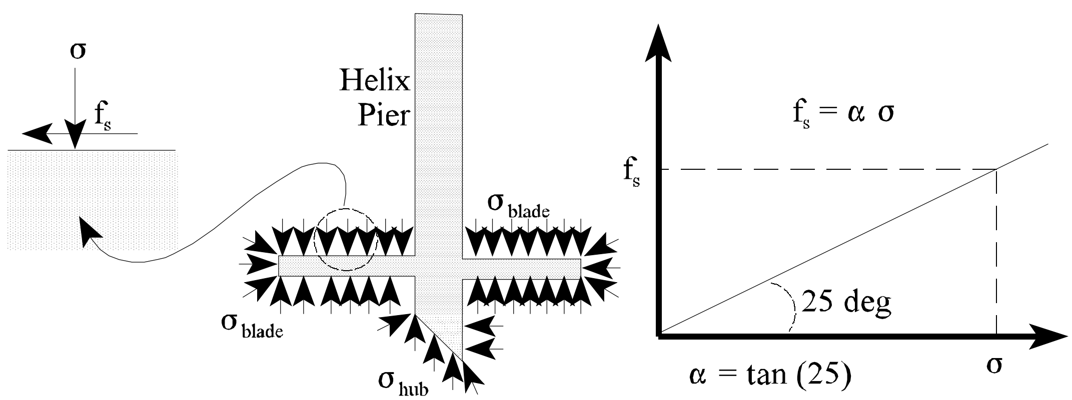

Fig. 5 Side Friction to Soil Penetration Resistance Relationship

Conclusions

A model was developed for determining the capacity/torque ratio for a helical foundation or anchor based on considerations of energy exerted during installation and that required to induce displacement once the helix pier is embedded in the soil.

Predictions based on the model correlate well with previous field and laboratory measurements. The model indicates that the capacity/torque ratio, K, is largely independent of downward force during installation, final installation torque, number of independent cutting blades, total number of helical blades, and blade pitch. The model indicates that K is moderately affected by helical blade radius and strongly affected by hub diameter and blade thickness. These predictions generally match measurements cited in previous literature.

Acknowledgments

The funding for this research program was provided by Secure Products, LLC. Appreciation is extended to Dr. Samuel P. Clemence of Syracuse University for his review and comments.

Nomenclature

"	ratio of side shear stress to penetration resistance
*	soil displacement during penetration (m)
)V	volume of soil displaced during penetration (m^3)
8	length of hub experiencing side friction (m)
N	internal angle of soil friction (deg)
F	penetration resistance (Pa)
A	penetrator area (m^2)
d	displacement during helix pier loading (m)
$E_{penetration}$	penetration energy (J)
$E_{installation}$	energy exerted during helix pier installation (J)
E_{losses}	energy lost due to side friction (J)
$E_{loading}$	energy exerted during helix pier loading (J)
F	downward force exerted during helix pier installation (N)
K	capacity/torque ratio
n	number of helical cutting blades
m	total number of helical blades
P	slope of soil stress-displacement constitutive relationship
r	radius of helix pier hub (m)
R_n	radius of n^{th} cutting blade (m)
R_m	radius of m^{th} helical blade (m)
t_n	thickness of n^{th} helical blade (m)
t_m	thickness of m^{th} helical blade (m)
T	installation torque (N-m)
Q	helix pier or anchor capacity (N)

References

A.B. Chance, Co. (1995). “Sample Calculations for Helical Pier Application.” Manufacturer Technical Support Document, Centralia, MO.

Clemence, S.P. (1985). “Uplift Behavior of Anchor Foundations in Soil.” *Proceedings of a Session Sponsored by the Geotechnical Eng. Div. of ASCE*, Detroit, MI.

Clemence, S.P. and Pepe, F.D. Jr. (1984). “Measurement of Lateral Stress Around Multihelix Anchors in Sand.” *Geotechnical Testing Journal*, GTJODJ, Vol. 7, No. 3, Sept. 1984, pp. 145-152.

Das, B.M. (1990) *Principles of Geotechnical Engineering*, 2nd Edition, PWS-Kent Publishing Company, Boston.

Ghaly, A., Hanna, A., and Hanna, M. (1991a). "Uplift Behavior of Screw Anchors in Sand. I: Dry Sand." *Journal of Geotechnical Engineering*, Vol. 117, No. 5, pp. 773-793.

Ghaly, A., Hanna, A., and Hanna, M. (1991b). "Installation Torque of Screw Anchors in Dry Sand" *Soils and Foundations*, Vol. 31, No. 2, Japanese Society of Soil Mechanics and Foundation Engineering, pp. 77-92.

Hargrave, R.L., and Thorsten, R.E. (1992). "Helical Piers in Expansive Soils of Dallas, Texas" 7th International Conference on Expansive Soils.

Hoyt, R.M. and Clemence, S.P. (1989). "Uplift Capacity of Helical Anchors in Soil." *Proceedings of the 12th International Conference on Soil Mechanics and Foundation Engineering*, Rio de Janeiro, Brazil.

Mitsch, M.P., Clemence, S.P. (1985). "The Uplift Capacity of Helix Anchors in Sand." Proceedings of a Session Sponsored by the Geotechnical Engineering Division, ASCE Convention, Detroit, MI, October 24, pp. 26-47.

Rao, S.N., Prasad, Y.V.S.N., and Shetty, M.D. (1991). "Behavior of Model Screw Piles in Cohesive Soils." *Soils and Foundations*, Vol. 31, No. 2, pp. 35-50.

Rao, S.N., Prasad, Y.V.S.N., and Veeresh, C. (1993). "Behaviour of Emebedded Model Screw Anchors in Soft Clays." *Geotechnique*, 43, No. 4, pp. 605-614.

Rupiper, S. and Edwards, W.G. (1989). "Helical Bearing Plate Foundations for Underpinning." Proceedings of Foundation Engineering Congress/SCE/CO Div., Evanston, IL, June 25-29.